Environmental Science & Technology

pubs.acs.org/est

Article

Informing the Exposure Landscape: The Fate of Microplastics in a Large Pelagic In-Lake Mesocosm Experiment

Chelsea M. Rochman,* Kennedy Bucci, Desiree Langenfeld, Rachel McNamee, Cody Veneruzzo, Garth A. Covernton, Gloria H. Y. Gao, Mira Ghosh, Rachel N. Cable, Ludovic Hermabessiere, Raul Lazcano, Michael J. Paterson, Michael D. Rennie, Rebecca C. Rooney, Paul Helm, Melissa B. Duhaime, Timothy Hoellein, Kenneth M. Jeffries, Matthew J. Hoffman, Diane M. Orihel, and Jennifer F. Provencher

Cite This: *Environ. Sci. Technol.* 2024, 58, 7998−8008

Read Online

ACCESS | Metrics & More | Article Recommendations | Supporting Information

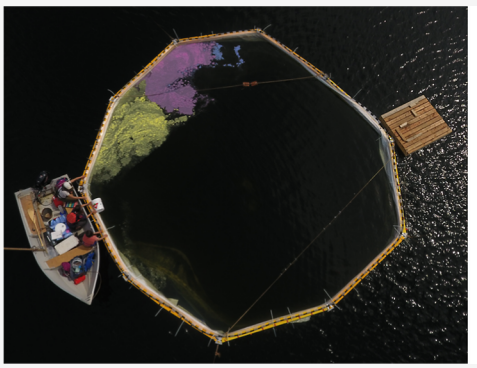

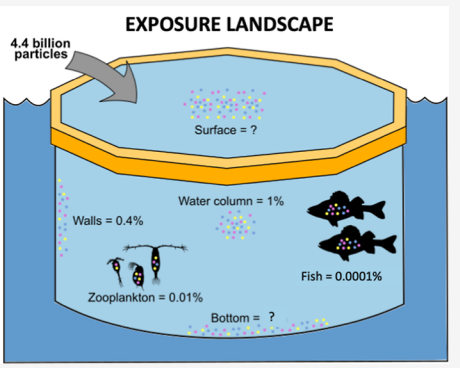

ABSTRACT: Understanding microplastic exposure and effects is critical to understanding risk. Here, we used large, in-lake closed-bottom mesocosms to investigate exposure and effects on pelagic freshwater ecosystems. This article provides details about the experimental design and results on the transport of microplastics and exposure to pelagic organisms. Our experiment included three polymers of microplastics (PE, PS, and PET) ranging in density and size. Nominal concentrations ranged from 0 to 29,240 microplastics per liter on a log scale. Mesocosms enclosed natural microbial, phytoplankton, and zooplankton communities and yellow perch (*Perca flavescens*). We quantified and characterized microplastics in the water column and in components of the food web (biofilm on the walls, zooplankton, and fish). The microplastics in the water stratified vertically according to size and density. After 10 weeks, about 1% of the microplastics added were in the water column, 0.4% attached to biofilm on the walls, 0.01% within zooplankton, and 0.0001% in fish. Visual observations suggest the remaining >98% were in a surface slick and on the bottom. Our study suggests organisms that feed at the surface and in the benthos are likely most at risk, and demonstrates the value of measuring exposure and transport to inform experimental designs and achieve target concentrations in different matrices within toxicity tests.

KEYWORDS: *transport, experimental design, freshwater, food web, ecotoxicity*

INTRODUCTION

Due to global transport via dust,[1] water,[2] and carbon[3,4] cycles, and like other persistent organic pollutants (POPs), microplastics are ubiquitous across ecosystems.[5,6] Within aquatic ecosystems, POPs (e.g., pesticides) partition based on hydrophobicity, informed by their molecular structure.[7,8] Microplastic particles, however, partition based on physical and chemical properties including surface chemistry, size, density, and shape.[9,10] As such, models that predict the fate and transport of POPs are not applicable to microplastics. Thus, new models must be developed to predict the fate and transport of microplastics, for which researchers are actively trying to determine the key structural parameters—e.g., size, density, shape, and the presence of biofilm.[11] Models that accurately predict the fate and transport of microplastics in the environment help us understand the exposure landscape, i.e., the pattern of contamination across an ecosystem that explains the concentrations to which organisms are exposed. An understanding of the fate and transformation of microplastics

Received: October 29, 2023
Revised: March 24, 2024
Accepted: March 25, 2024
Published: April 17, 2024

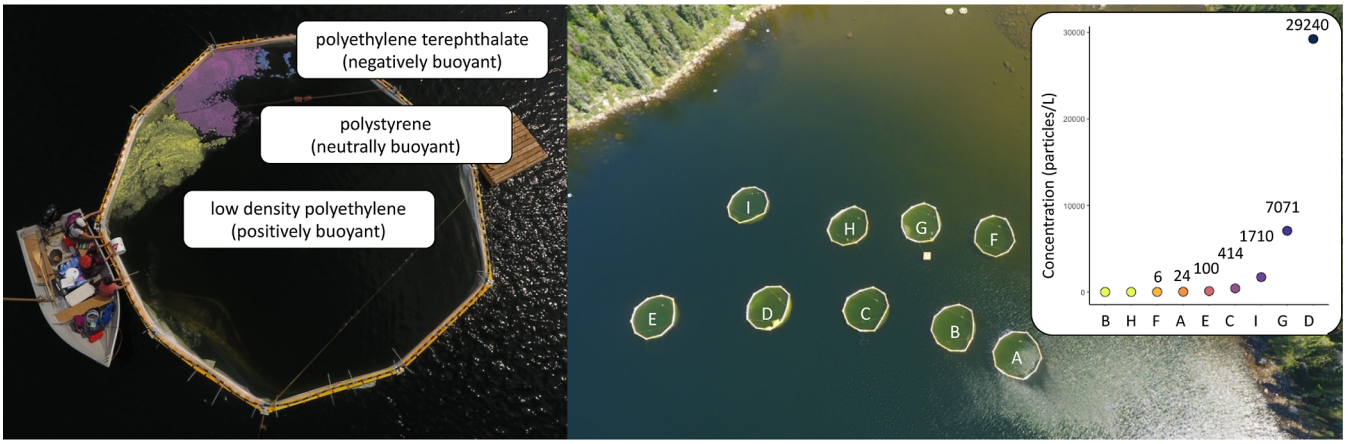

Figure 1. Left: close-up drone image of mesocosm G showing the three types of microplastics as they are being added. The different polymer types are labeled (with their relative densities) next to the slicks of each, differentiated by color (blue is polyethylene terephthalate, pink is polystyrene, yellow is polyethylene). Right: a drone image of all nine mesocosms and a plot showing the nominal water concentrations (*y*-axis) within each mesocosm (*x*-axis). Photo credit: Dr. Scott Higgins.

is critical to informing predictions about where plastics will accumulate in the environment, exposure to wildlife, and improved methods for toxicity testing and risk assessment.

Several studies have tested hypotheses, theories, and predictions about the fate and transport of microplastics within and across matrices, using tools such as environmental sampling, laboratory and field experiments, or computer modeling. Environmental sampling campaigns can be used to understand the distribution of microplastics in surface waters,[12] the water column,[13] sediments,[14,15] and biota.[16,17] Although these studies provide useful information about the fate of microplastics, in isolation, they are insufficient for informing a mass-balance approach. Laboratory experiments are also employed to test hypotheses about fate and transport, using tanks and columns to measure processes such as sinking,[18] resuspension,[19] degradation,[20] and others. While these studies lack real-world complexity (e.g., biofouling, temperature fluctuations, turbidity, etc.), they provide important information that can be used to construct predictive models. Similarly, in silico models also lack real-world complexity but are useful for building hypotheses and predictions about transport processes of microplastics,[21] global contamination patterns,[22] mass-balance,[23] and transformations (e.g., fragmentation[24]). In the present study, we used large-scale field experiments to test hypotheses about fate and effects. Large-scale experiments in nature are critical for understanding contaminants, as they inherently capture environmental relevance within the experimental design. Although they are less common due to the resources (cost, time, personnel) and permissions needed, they are powerful for demonstrating the fate, transport, and ecological effects of anthropogenic stressors,[25−28] and informing policies that protect ecosystems and human health.[29] Recognizing the value of large-scale experimental research, Canada's government set aside 58 lakes and their watersheds for research, creating the Experimental Lakes Area in Northwestern Ontario.[29] For more than 50 years, scientists have been using this unique research station to answer questions about the fate and effects of anthropogenic stressors in aquatic ecosystems, including eutrophication,[30] climate change,[31] acid rain,[32] pharmaceuticals[25] industrial chemicals,[33] and crude oil.[34]

In June−August 2021, we conducted an in-lake mesocosm experiment with microplastics at the International Institute for Sustainable Development's Experimental Lakes Area (IISD-ELA). The objectives of our entire experiment include the fate and transport of microplastics as well as the ecological effects on individuals, populations, and communities. In this paper, we introduce the experiment and present only the results documenting the transport and fate of microplastics in the water column, in biofilm on the mesocosm walls, in zooplankton, and in the gastrointestinal tracts (GITs) of fish. In future papers, we will describe the effects on biota and the fate of the additive chemicals. Our objectives relevant to this paper were to determine the exposure landscape to fish and other organisms in our experiment by (1) measuring how microplastics partition across matrices (i.e., water and biota) within our mesocosms and (2) measuring how fate and transport vary among polymer types and sizes—all to inform the microplastic exposure landscape to organisms in nature (i.e., the realized concentrations). Our hypotheses were that realized concentrations would vary across the mesocosms based on the size and density of the microplastics. We predicted that denser and larger particles would sink more rapidly than smaller and less dense particles. This experiment is part of the "pELAstic" project, a decade-long research program consisting of increasingly complex experiments designed to better understand the fate and effects of microplastics in freshwater ecosystems across multiple spatial, temporal, and ecological scales. This work is the first of a series of pELAstic project-related articles for this pelagic mesocosm experiment. Future articles will describe observations relevant to the fate of additive chemicals, the biological fate of microplastics, the transformation of microplastics, and biological and ecological effects.

METHODS

Experimental Design. The experiment took place over a 10-week period at the IISD-ELA, near Kenora, Ontario, Canada (49°40′N, 93°44′W). Nine mesocosms were deployed along the northwestern side of lake 378 (Figure 1), a typical oligotrophic headwater Canadian Shield boreal lake with a surface area of 25 ha, a volume of about 1.8 million m^3, and a maximum depth of 18.2 m. Each mesocosm was anchored in

https://doi.org/10.1021/acs.est.3c08990
Environ. Sci. Technol. 2024, 58, 7998−8008

the pelagic zone in an area that ranged from 3 to 6 m in depth. The mesocosms were cylindrical and closed-bottom (10 m diameter, 2 m depth), constructed using 8 mm-thick, food-grade, low density polyethylene (Curry Industries, Winnipeg, MN, Canada) attached to a floating vinyl-wrapped expanded polystyrene decagonal ring (Dow, Midland, MI, USA) held together on the outside by malleable polyvinyl chloride piping and zip ties. Each mesocosm was held in place by anchors from the ring to the lake bottom via concrete weights attached using a manila rope. Mesocosms were positioned 2−3 m apart and were suspended off the bottom, except for one (mesocosm F, see Figure 1) that drifted during a storm near the beginning of the experiment and was touching the lake bottom.

Each mesocosm was filled with ∼150,000 L of lake water pumped from ∼1 m depth via a trash pump (Honda Canada) connected with a fire hose. Microbial, phytoplankton, and zooplankton communities from lake 378 were pumped into each with the water. To offset potential mortality from pumping, we added zooplankton to each mesocosm by collecting fifteen 10 m vertical hauls per mesocosm using a 0.5 m diameter net with 150 μm mesh. Before adding microplastics, we allowed the communities to acclimate for 2 weeks. During acclimation, we collected yellow perch (*Perca flavescens*), roughly 70−100 mm in length, from lake 378 and added 25 fish per mesocosm, which matched the natural density of this species (approximately 3000 fish per ha) in a nearby reference lake (lake 239).[35] Fish were collected using trap nets and seining under a collection permit from the Ontario Ministry of Natural Resources (MNR; 1097798) and an animal care permit from the University of Toronto (20012583). Due to challenges collecting fish, and higher than expected mortality, the number of fish that survived across mesocosms was not equal (Table S1). Although fish fed on their natural prey in the mesocosms (i.e., primarily zooplankton), we supplemented their diet to ensure an adequate food supply in the mesocosms. Fish were fed commercial frozen mysis shrimp (every 3 days) at a rate of 2% fish body mass per day initially, which was reduced to roughly 0.8% of the body mass per day by the end of the experiment as the fish grew. This range represents field-based estimates of consumption for this species.[35,36] Densities of fish were monitored at irregular intervals throughout the experiment using a remotely operated vehicle (Open ROV Trident), and feeding rates were adjusted to reflect the estimated fish densities in each mesocosm.

Microplastics were added to seven of the nine mesocosms as a single addition on June 2, 2021. Two negative control mesocosms were included to account for the natural variability among mesocosms. Our experimental design consisted of a regression design on an approximate log scale, targeting nominal concentrations of 6, 24, 100, 414, 1,710, 7,071, and 29,240 microplastic particles/L (Figure 1). Nominal concentrations are relevant to those reported in freshwater ecosystems[37] when rescaled to account for a broader particle size distribution using methods by Koelmans et al.[38] and Kooi et al.[39] The microplastics used in our experiment were an equal mixture (by count) of fragments of yellow PE (linear low density polyethylene, density = ∼0.93 g/cm^3), pink PS (polystyrene, density = ∼1 g/cm^3), and blue PET (polyethylene terephthalate, density = ∼1.4 g/cm^3). The plastics were custom-made by TechmerPM (Batavia, IL, USA) and ground into microplastics by the Custom Processing Service (Reading, PA, USA). The size of the PE particles ranged from 37 to 1086 μm (average: ∼209 μm), the PS particles ranged from 48 to 1408 μm (average: ∼197 μm), and the PET particles ranged from 52 to 1408 μm (average: ∼232 μm; see Supporting Information text and Figure S1 for more details on particle size distributions). Each polymer type had its own suite of chemical dyes and additives (Table S2). The amount of microplastics added per mesocosm was determined using a mass to count relationship determined for each polymer (see Supporting Information text, Table S3, and Figures S2−S4 for more details). Microplastics were added to the mesocosms by first wetting the plastics (to reduce loss via wind) by fully submerging each type in a slurry of mesocosm water within a falcon tube, jar, Ziplock bag, or bucket (depending on the treatment) and then manually mixing and releasing the slurry just below the surface of the water to ensure deployment within the mesocosm.

Water Quality and Chemistry. We monitored water temperature, conductivity, dissolved oxygen, and turbidity weekly and photosynthetically active radiation (PAR) on weeks 0, 1, 2, 3, 4, 6, 7, 9, and 10, from each mesocosm during the experiment. Water chemistry samples were taken on four sampling dates (starting before the exposure began) and at weeks 2, 6, and 10. Samples were taken from every mesocosm on each sampling event, except for weeks 2 and 6 when we took samples from only three mesocosms (Ctrl-2, 100 particles/L, and 29,240 particles/L). Water quality and chemistry parameters were generally similar among treatments and did not consistently vary with nominal microplastic concentrations (Tables S5−S8). Parameters did vary with time across all mesocosms, as can be expected due to natural variation. However, light penetration (PAR) was positively correlated with microplastic concentration at multiple time points. Further details regarding sampling methods and results are in Supporting Information.

Microplastic Fate Sample Collection. We sampled the water column, biofilm growing on the mesocosm walls, zooplankton, and fish. We quantified and characterized (i.e., polymer type and size) microplastics in each of these matrices to determine the concentration and size distribution of the three polymers across different parts of the lake ecosystem enclosed by the mesocosms.

In the water column, water was collected at 10 cm, 1 m, and 2 m depths at 24 and 72 h, as well as 1, 2, 3, 4, 6, 8, and 10 weeks after the addition of microplastics. One sample was taken from each depth within each mesocosm at each sampling period. These depths were sampled to determine whether the microplastics in the water column were well-mixed or if there was variability across the depths. Four L of water was sampled from each depth using a peristaltic pump (GeoTech; Denver, CO, USA) with 6.35 mm Tygon tubing and inline filtration. The filters were 47 mm in diameter and were made of polyester mesh (Spectrum Med, Toronto, ON, Canada) with a 10 μm pore size. The samples taken from the control mesocosms served as field blanks. Immediately after sampling, the filters were placed in clean plastic Petri dishes. To avoid any interference from the walls of the mesocosm, the sampling tubes were fed through holes drilled into a cork yoga block that was clipped onto a manila rope line secured across the mesocosm. The cork block was pushed roughly 1 m from the walls of the mesocosm prior to water sampling. After sampling, filters were agitated by hand in 250 mL of reverse osmosis (RO) water to release microplastics. The RO water was topped

https://doi.org/10.1021/acs.est.3c08990
Environ. Sci. Technol. 2024, 58, 7998−8008

with a capful of 99% isopropyl alcohol and stored in clean polypropylene jars at room temperature until analysis.

For biofilm, we deployed strips of wall material (1.5 m × 10 cm) from manila rope 1 m from the walls and weighted them at the base to maintain their orientation in the water column. Three strips were deployed at the beginning of the experiment, and we collected one at each of 3, 6, and 9 weeks. The strips were collected and sectioned into 10 cm lengths in the field for different analyses. The sections from 0.20 to 0.30 and 1.20 to 1.30 m depth were retained for microplastic quantification. Strips were transported from the field in glass bottles to the laboratory for processing.

We sampled zooplankton from each mesocosm using a Wisconsin plankton net with a 0.25 m diameter opening and a 53 μm mesh during week 10 of the experiment. Two 1.5 m vertical net hauls were collected from opposite sides of each mesocosm to ensure a representative sample (total sample volume of 147 L) and preserved in 5% sugar-formalin[40] after narcotization in methanol.[41]

We sampled fish from each mesocosm at the end of the experiment using a seine net (6.4 mm mesh, 2 m height, and 30.5 m in length). Fish were euthanized with MS-222. Fish in each mesocosm were used for multiple end points, and thus only 1−7 fish from each mesocosm were used to quantify microplastics.

Microplastic Fate Sample Processing. Due to time and resource constraints, microplastics were extracted and analyzed in samples collected from one control mesocosm at the 24 h and 10-week periods (as a measure of QA/QC), and three of the nine plastic treatments for all sampling periods with target nominal concentrations of 6 (low), 414 (medium), and 29,240 (high) particles per liter. Here, we report on microplastics >53 μm in size—which is close to the low end of the size distribution of each of the polymers added.

Microplastics were extracted from water samples collected at each time point via sieving. Samples were size fractioned by running each water sample through a stainless-steel sieve stack with 212, 106, and 53 μm pore sizes. Each size fraction (>212, 106−212, and 53−106 μm) was rinsed with RO water into a clean glass mason jar.

Biofilm on the wall material was extracted from the strips via a combination of vigorous agitation in glass bottles and scraping with sterile, disposable Corning cell lifters made of white PE followed by triple-rinsing with distilled water. The resulting biofilm slurry was filtered through a 47 mm GF/F filter and placed in a polypropylene specimen cup with RO water, sonicated for 1 h, and placed into 50 mL of digestion solution (30% H_2O_2) loosely covered with tinfoil. Samples were digested in solution at 45 °C for 48 h. Following digestion, samples were sieved and stored as described above for water samples.

Microplastics were extracted from zooplankton from each of the four mesocosms and two procedural blanks consisting of RO water. From each mesocosm, 5−100 individuals were picked under a microscope using fine metal forceps for each of the five most common species: *Diaphanosoma birgei*, *Diaptomus minutus*, *Eubosmina* sp., *Mesocyclops edax*, and *Tropocyclops extensus*. To remove microplastics that may have been attached to the outside of the zooplankton, each sample was rinsed with RO water over a metal mesh sieve before digestion. Each sample was then rinsed into a clean polypropylene jar with 30% H_2O_2, digested at 45 °C for 48 h, and sieved as described above.

Microplastics were extracted from fish and 12 procedural blanks consisting of RO water. Fish were dissected, and the GITs were removed and stored in individual pre-cleaned polypropylene specimen cups. Each GIT was digested in 20% KOH for 24−48 h at 45 °C and sieved through a 53 μm stainless steel sieve. The contents on the sieve were then filtered onto a 10 μm pore size, 47 mm diameter polycarbonate filter.

Microplastic Counting and Characterization. Microplastics were manually quantified and characterized in each sample under a dissection microscope. Briefly, each sample was sorted wet (except for fish), taking one spoonful at a time into a clean glass Petri dish and systematically assessing the whole dish. When the full jar was sorted, it was triple rinsed with RO water, and the rinsewater was also assessed for microplastics. Fish samples were sorted dry on filters, scanning the full filter systematically. When a suspected microplastic particle was identified, it was recorded by color (blue = PET, pink = PS, yellow = PE). The first 10 particles of each color within each size fraction were picked with forceps and mounted on double-sided tape. When particles looked like the PE, PS, or PET we added but the color could not be clearly identified (usually when particles were very small), the first 20 suspected microplastic particles of unknown color were picked and mounted on double-sided tape. Because there were very few unknown particles, we generally picked them all. The picked particles created a subsample that could be measured and chemically analyzed to confirm the polymer type.

Because we spiked our mesocosms with brightly colored microplastics, we did not perform spectroscopy on picked particles across all samples. First, we tested the accuracy of our researchers (n = 8 researchers) for picking the PE, PS, and PET particles from three samples. For these three samples, all picked particles suspected to be PE, PS, or PET were analyzed via Raman spectroscopy (water, biofilm, zooplankton) or μ-FTIR (fish). If accuracy was >70%, we only performed spectroscopy on the picked particles labeled unknown where there was less confidence regarding color. For chemical identification, we predominantly used μ-Raman spectroscopy (Xplora Plus, HORIBA, Piscataway, NJ, USA) operated with LabSpec6 software and a 785 nm (range 50−2000 cm^{-1}) laser with spectral library databases (including SLoPP and SLoPP-e[42]) and matching software (Bio-Rad KnowItAll and ID Expert). For particles in fish, we used a Nicolet iN10 Infrared Microscope (Thermo Fisher Scientific) in attenuated total reflectance (ATR) mode (15× objective, 0.7 numerical aperture) with a germanium ATR crystal. The spectral library used was Opus and the μ-ATR−FTIR Spectral Library of Plastic Particles (FLoPP and FLoPP-E).[43] For further information, see Supporting Information.

Average accuracy for each researcher (n = 8) ranged from 73 to 92%. Thus, we only performed Raman spectroscopy on the picked suspected particles of unknown color in all water, biofilm, and fish samples. For zooplankton, where there were generally less than 10 particles per sample, we chemically analyzed all particles and spectroscopy-corrected the data set. For water samples, 21.6% of suspected microplastics of unknown color were confirmed to be PE, PS, or PET. As such, we spectroscopy-corrected the sum of unknown particles in each sample by multiplying by 0.216. For biofilm, 29.1% of the suspected microplastics of unknown color were confirmed to be PE, PS, or PET, and we spectroscopy-corrected the sum of unknown particles in each sample by multiplying by 0.29.

https://doi.org/10.1021/acs.est.3c08990
Environ. Sci. Technol. 2024, 58, 7998−8008

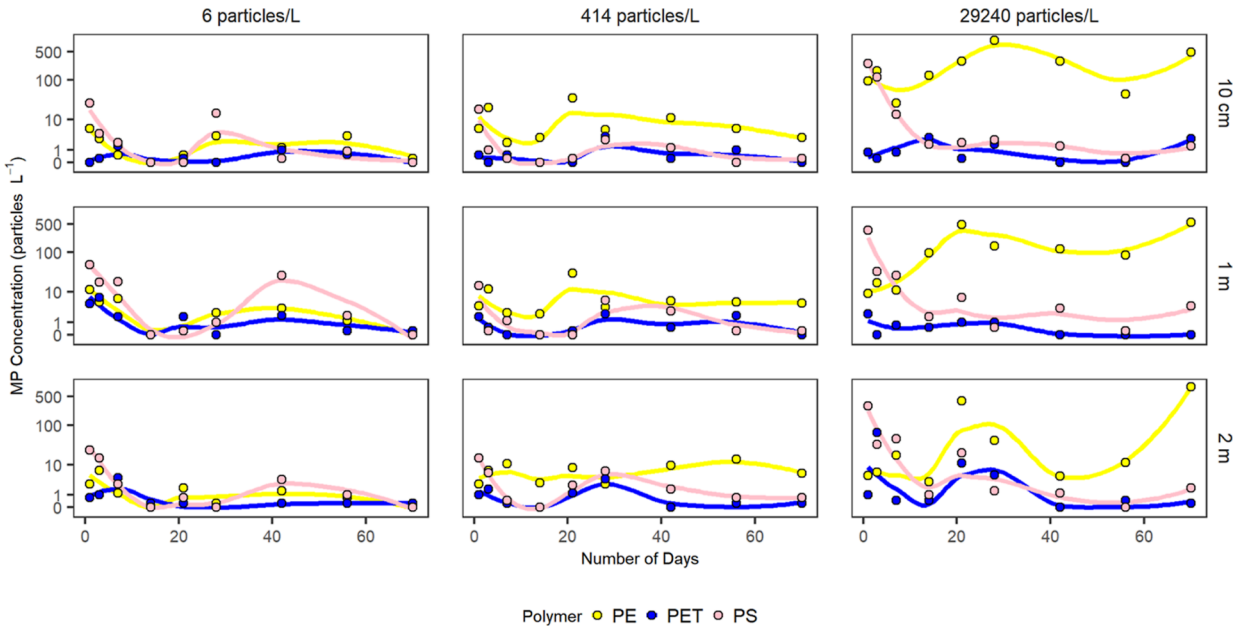

Figure 2. Concentrations of microplastics in the water column of the 6 (left), 414 (center), and 29,240 (right) particle per liter treatments. Concentrations are on a log-scale (*y*-axis) and are reported for each polymer type (PE—yellow (positively buoyant), PET—blue (negatively buoyant), PS—pink (neutrally buoyant)) over time (*x*-axis) and at each sample depth (10 cm—top, 1 m—middle, 2 m—bottom). The colored lines are local polynomial regression smoothers fit using the loess function in R to aid with visualization.

For fish, 58% of the suspected microplastics of unknown color were confirmed to be PS or PET, and because we performed spectroscopy on all unknown particles detected, we spectroscopy-corrected the unknown particles in each sample. These corrected unknown particle sums were added to the total microplastic particle sums for each sample (versus added to the sums for each polymer).

Quality Assurance/Quality Control. To account for and limit procedural contamination, our experimental design included color-labeled microplastic fragments of known polymer and chemical composition. Where possible, we avoided equipment (e.g., ropes and sampling equipment) with these colors. All sampling equipment, sample containers, and dishes were triple-rinsed with RO water or ambient lake water for larger equipment (e.g., water samplers) before use and between samples (to minimize cross-contamination). In the field, samples were collected in order of lowest to highest microplastic concentrations. Where possible, different equipment was used for controls versus microplastic treatments (e.g., a water sampling device). In the laboratory, care was taken to wear white cotton laboratory coats, keep samples covered to protect them from dust, and conduct processing in a room with a HEPA filter. Samples collected from the control (0 particles/L) mesocosm helped track procedural contamination. Brief results from the control mesocosm are presented in the Results Section, and detailed observations can be found in Supporting Information Results and Data. For zooplankton and fish, we also analyzed two and 12 procedural laboratory blanks, respectively. The laboratory blanks (consisting of RO water) mimicked sample processing relevant to all laboratory procedures (e.g., dissection, digestion, and sorting). In total, we found only one PE particle in a procedural blank. Because we are most interested in patterns over time and across mesocosms, final data presented here are not recovery- or blank-corrected. Particle counts are spectroscopy-corrected as described above. Recovery tests and rates for our laboratory analyses are reported in Supporting Information.

Data Analysis. To explore how microplastic size and polymer type affected the temporal fate of particles, we used generalized linear models for each polymer type from the mesocosm with the highest microplastic concentration. All data analyses were conducted using R v4.2.2.[44] We used the glmmTMB package for all linear modeling.[45] To determine the best model for each polymer, we began by fitting models with day of experiment as a continuous predictor and size fraction and depth as categorical predictors, including all 2-way and 3-way interactions. For each polymer, we fit a Poisson model then checked the simulated residual diagnostics via the DHARMa package.[46] The models were poor fits; therefore, negative binomial models with linear variance formulation were tried. For the polymers where the residual diagnostics were still poor, a negative binomial with quadratic formulation model was used. For all models, we used microplastic count as the response variable, and the log-transformed volume of water sampled was included as an offset term to account for sample volume while keeping the response as integer data. For the PS model, none of the 3-way interaction models fit, so 2-way interaction models (with all possible interactions) were fit. It was necessary to log-transform the number of days only in its interaction with size fraction to solve issues with residual heterogeneity. Once the appropriate distribution was selected, likelihood ratio tests were used to compare each full model to a model with 2-way interactions. If the *p*-value was not significant (α = 0.05), the 2-way interaction models were interpreted if simulated residual diagnostics were still acceptable. To interpret effects, we used the emmeans and ggeffects packages to calculate and visualize model estimated marginal means alongside the collected data.[47,48]

https://doi.org/10.1021/acs.est.3c08990
Environ. Sci. Technol. 2024, 58, 7998−8008

RESULTS AND DISCUSSION

Microplastic Concentrations in the Water Column. We sampled water from three depths and over time to determine the exposure landscape of microplastics in the water column (Figure 2). In the highest nominal concentration treatment (29,240 particles/L), we observed an overall mean (±stdev) concentration (across all depths and sampling periods) of 246 (±202) particles/L), ranging from 48 to 631 particles/L (with no clear pattern over time). This is 2 orders of magnitude less than the nominal concentration and ∼1% of the particles we added to the mesocosm, indicating that the majority of the microplastics were in other environmental compartments (e.g., on the water surface, at the bottom, in biofilm on the walls) or potentially escaped the mesocosms via wind and wave action. For each polymer type within the 29,240 particles/L mesocosm, mean (±stdev) concentrations (and percentage of the total addition by count) in the water over time and across depths were 196 (±214) particles/L PE (2% of PE added by count), 45 (±97) particles/L PS (0.5% of PS added by count), and 4 (±7) particles/L PET (0.04% of PET added by count). For the 414 particle/L mesocosm, patterns were similar, and we observed a total mean (±stdev) concentration of 13 (±8) particles/L, which is 3% of the total particles we added to the mesocosm. For each polymer type within the 414 particles/L mesocosm, mean (±stdev) concentrations (and percentage of the total addition) over time and across depths were 8 (±7) particles/L (6%), 3 (±5) particles/L (2%), and 1 (±1) particles/L (0.6%) of PE, PS, and PET in the water column, respectively. For the 6 particle/L mesocosm, the number of particles in the water column was higher than expected, with a mean (±stdev) total concentration, across time and depths, of 12 (±14) particles/L. This is equivalent to 201% of the particles we added to the mesocosm by count, i.e., higher than the nominal concentration. For each polymer type within the 6 particle/L mesocosm, mean (±stdev) concentrations (and percentage of the total addition), over time and across depths, were 2 (±2) particles/L (124%), 8 (±11) particles/L (395%), and 1 (±1) particles/L (53%) of PE, PS, and PET in the water column, respectively. For the control mesocosm, we observed average concentrations of 2.7 and 1.3 microplastic particles/L across sampling depths at 24 h and 10 weeks, respectively. The higher concentration detected in the 6 particle/L mesocosm may be due to cross-contamination between mesocosms via sampling equipment. It is also possible that our sampling method was not representative for this treatment; i.e., the volume sampled was not enough to representatively sample the lower concentration (which based on the two treatments above, we might expect ∼0.1 particles/L). In the future, we will take duplicate samples to measure the precision of our sampling methods.[49]

The relative distribution of polymer types in the water column was similar across treatments (Figure 2), so we discuss patterns related to time, depth, and particle size for each polymer type using data from the mesocosm with the highest nominal concentration. Based on equations from Waldshlager and Schuttrumpf et al. (2019),[18] the density of the polymers, and assuming a density of 1 g/cm^3 for freshwater and using an approximate water temperature of 20 °C, we can estimate settling velocities for the particles added to our mesocosms. Here, we include different morphologies, using Corey shape factors,[50] because our particles range from relatively spherical to fibrous (Figure S1). The density of PE is less than 1 g/cm^3, and thus, we expect it to float. For larger particles of PS and PET, that are more spherical in shape and roughly 350 μm in size, we estimate a settling velocity of 1.7 and 13.8 mm/s, respectively (i.e., larger particles of PS and PET would be expected to reach the bottom of our 2 m mesocosm in less than 1 h). For smaller particles (53 μm) that are more fibrous in shape, which is typical of our particles, we would predict settling velocities of 0.0028 mm/s for PS and 0.033 mm/s for PET. Based on this, for smaller PS and PET particles, we would expect them to reach the bottom in 8.2 days and 15.6 h, respectively.

Due to observations in laboratory experiments that measure settling velocities of buoyant particles,[51] we did not expect all of the PE particles to remain at the surface over the experiment. Particle concentrations of PE increased over time at all depths for the 106−212 and >212 μm size fractions only (Figure S8). There was a strong effect of depth, with more particles in the 10 cm samples over time compared to the other depths. The results suggest that PE particles primarily floated in the water column with most near the surface throughout the experiment. Anecdotally, we could visually see PE at the surface (as a microplastic slick) that decreased in size and density over time. The relatively consistent concentration of particles over time at a depth of 10 cm may have been due to a continuous sinking of particles from the surface slick. Moreover, the increasing concentrations of larger particles over time in the water column may have been due to biofouling of these buoyant particles changing their density toward negatively buoyant.[51] For PE, the negative binomial with linear variance formulation GLM was the best fit (Figure S8). The 3-way interaction was not significant ($p > 0.05$) so the 2-way model was interpreted. Only the time and size fraction interaction was significant ($p = 0.04$).

For PS, there were more smaller particles initially at all depths, and particle concentrations decreased exponentially over time for all depths and size fractions, suggesting ongoing deposition (Figure S9). Most of the particles added to the mesocosms were not within the smaller size fraction, so the pattern of smaller particles initially may be due to the timing of our first sampling. At 24 h, most of the larger particles of PS may have already settled to the bottom, as predicted. Smaller particles reached the bottom slower, within roughly 1−2 weeks (Figure S9). The model suggests that PS particle concentrations across size fractions at the different depths were similar by 1 week. For PS, the negative binomial GLM with linear formulation of variance for the 2-way interaction model was the best fit (Figure S9). There were significant interactions between time and size fraction ($p < 0.001$) and time and depth ($p = 0.001$).

As confirmed by visual observation, and as predicted based on calculations, most PET particles (of all sizes) sank immediately and were not observed on the surface after the initial additions (i.e., from 24 h onward). For PET, the negative binomial GLM with a quadratic variance formulation was the best fit. The 3-way interaction was not significant, but the 2-way interaction model did not pass residual diagnostics, so the 3-way model was interpreted. The main prediction of the model was higher PET concentrations at 2 m depth within the first week (Figure S10). However, this prediction was mostly driven by one sample with high concentrations, as the particle concentrations were close to zero for most other water samples.

https://doi.org/10.1021/acs.est.3c08990
Environ. Sci. Technol. 2024, 58, 7998−8008

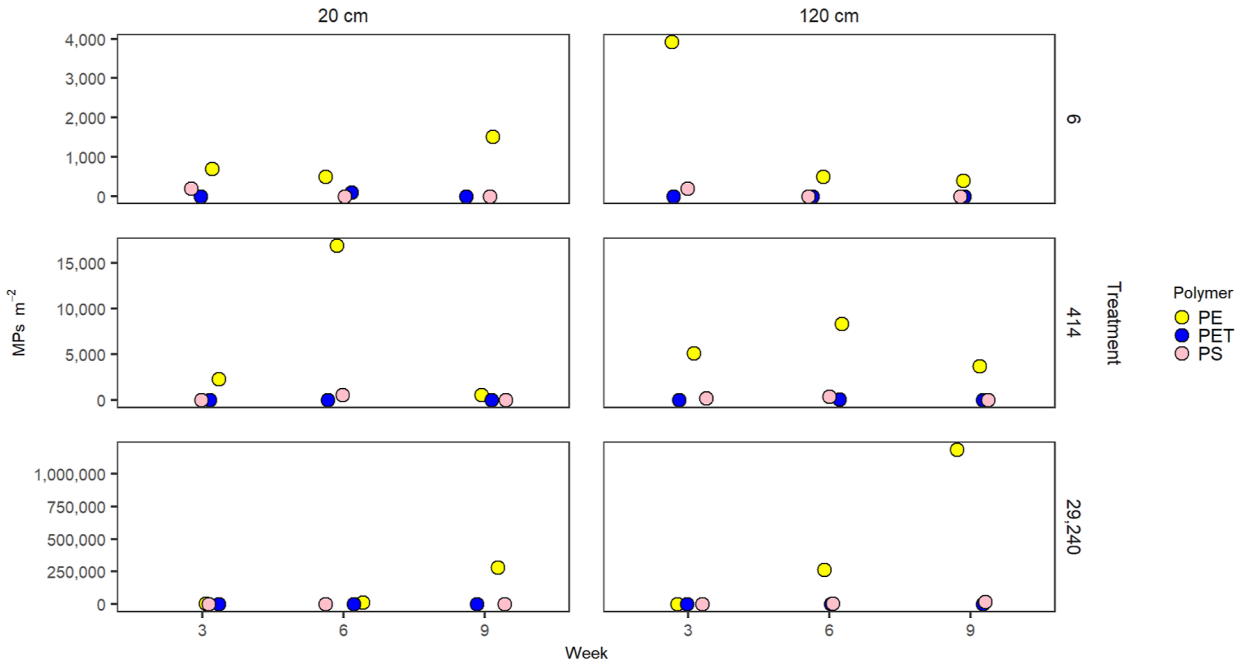

Figure 3. Concentrations of microplastics (y-axis; particles/m^2) on the wall strips for each type of microplastic (PE = yellow, PET = blue, PS = pink), at 3-, 6-, and 9-week sampling periods (x-axis) within the 6, 414, and 29,240 particle/L treatments (rows) and at each depth (columns). Note the differences in the y-axis among the treatments.

Overall, total concentrations of microplastics in the water column were much lower than nominal concentrations, and there were clear patterns with depth for each polymer type. Denser particles were less abundant than buoyant particles. Moreover, there were more smaller particles than larger particles (as observed for PE and PS). Visual observations confirmed these patterns in the data. We witnessed the PET microplastics sinking rapidly upon addition, while the neutrally buoyant particles (PS) sank gradually over time. For buoyant PE, we observed a slick at the surface that was not quantified by our sampling. The slick diminished over time, likely replenishing microplastics in the water column as they slowly sank to the bottom of the experiment. The larger and denser particles, similar to what was observed by Hoellein et al.[28] and Elagami et al.,[52] likely sank to the bottom quickly, and stayed there.

Microplastics in Other Matrices. Generally, across mesocosms, we observed that the amount of microplastics in the wall-attached biofilm within each mesocosm increased with an increasing nominal concentration (Figure 3). Although, the concentrations in the lowest (6 particles/L) and mid (414 particles/L) nominal concentration mesocosms were consistent from week 3 to week 9, microplastics appeared to increase through time in the biofilm within the mesocosm with the highest nominal microplastic concentration (29,240 particles/L). At the 0.2 m depth, total concentrations in biofilm from the highest nominal concentration treatment were 6411, 15,229, and 282,907 particles/m^2 at 3, 6, and 9 week, respectively. At the 1.2 m depth, they were 1642, 270,483, and 1,205,310 particles/m^2 at 3, 6, and 9 week, respectively. Most of the particles in the biofilm, in general, were PE. At the 0.2 m depth, PE particles made up 92−99.5% of particles, PS particles made up 0.5−2%, and PET particles made up 0−2%. At the 1.2 m depth, PE particles made up 92−99% of particles, PS particles made up 1−6% of particles, and PET particles made up 0−0.01% of all particles. At both depths, the concentration of PE and PS in biofilm in the highest nominal concentration treatment increased at each sampling period. PET, in contrast, was consistent from week 3 to week 6, then in week 9, the concentration of PET in biofilm at the 0.2 m depth dropped with a concomitant increase at the 1.2 m depth, indicating that PET may have sunk vertically through the biofilm via gravity. Patterns across treatments are shown in Figure 3 and concentrations in the medium and lowest nominal concentration treatments are given in Supporting Information Data. In the control mesocosm, we observed an average of 468 microplastic particles/m^2 across depths at the 3 week sampling period, and an average of 5192 microplastic particles/m^2 at the 9 week period. Patterns of microplastic concentrations in the wall-attached biofilm were similar across particle sizes (Figure S11). The pattern of accumulation through time, evident in the highest treatment mesocosm only, was perhaps not apparent in the low and medium concentration mesocosms due to the lower availability of microplastics in the water column. For example, within the medium nominal concentration treatment, there were <30 particles/L suspended in the water column by week 9 (Figure 2). As particles settled to the bottom of the mesocosms, the supply of particles to become entrapped in the biofilm on the mesocosm walls would become limited, and losses from biofilm sloughing or from the downward migration of microplastics through the biofilm would not be replaced. What bears further investigation is the maximum capacity of the biofilm to take up microplastics from the surrounding water.

Across all zooplankton, there was a mean (±stdev) of 0.06 (±0.07) particles per individual in the highest nominal concentration mesocosm (29,240 particles/L), 0.07 (±0.08) particles per individual in the medium nominal concentration mesocosm (414 particles/L), and 0.01 (±0.01) particles per individual in the lowest nominal concentration (6 particles/L) mesocosm. Within the control mesocosm, there was an average

https://doi.org/10.1021/acs.est.3c08990
Environ. Sci. Technol. 2024, 58, 7998−8008

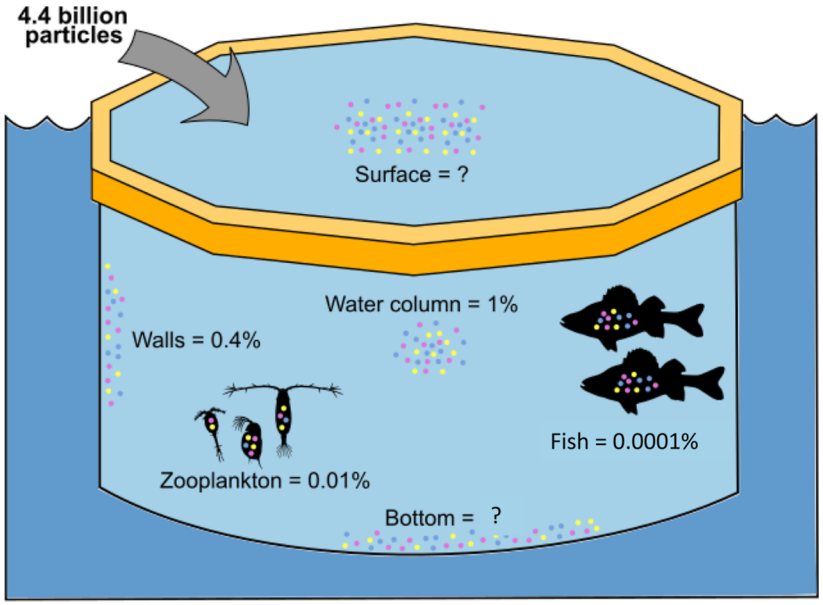

Figure 4. Exposure landscape, showing the average percent (over time and across depths where relevant) of the total plastic added to the highest concentration mesocosm in each sampled compartment within the mesocosm.

of 0.02 microplastic particles per individual. Similar to other matrices, the amount of microplastics in zooplankton from the lowest nominal concentration mesocosm compared to the control suggests that we should have sampled more individuals per sample to get a more accurate value. We found microplastics in all five taxonomic groups that were analyzed. Zooplankton primarily ingested PE and PS, which correspond to their greater availability in the water column. In the highest concentration treatment, mean microplastic composition in zooplankton was 46% PE, 54% PS, and 0% PET. In the medium concentration treatment, mean microplastic composition was composed of 19% PE, 81% PS, and 0% PET. In the lowest concentration treatment, mean microplastic composition was composed of 60% PE, 40% PS, and 0% PET. Detailed information about concentrations and patterns observed per taxa will be included in a separate manuscript.

In fish, there was a mean (±stdev) of 581 (±37) total microplastic particles per individual (n = 2) in the highest nominal concentration mesocosm, 12 (±1) particles per individual (n = 3) in the medium nominal concentration mesocosm, and 1 (±0) particle per individual (n = 2) in the lowest nominal concentration mesocosm. In the control mesocosm, the average total amount of microplastics per individual was 3 (n = 8). Microplastic abundance in fish follows the same ordinal pattern of the nominal concentrations in the mesocosms. This is consistent with other studies that show that the amount of microplastics in fish correlate with exposure concentrations.[53] We observed fish ingesting all three polymers, with patterns varying across treatments. In the highest concentration treatment, mean microplastic composition in fish was 77% PE, 21% PS, and 2% PET. In the medium concentration treatment, mean microplastic composition in fish was 28% PE, 47% PS, and 25% PET. In the lowest concentration treatment, mean microplastic composition in fish was 0% PE, 50% PS, and 50% PET. Because the GIT samples include the dense PET and PS, which more rapidly settled out of the water column, our data suggest that fish were feeding throughout the mesocosms, including at the bottom. Detailed assessments of the microplastics in the fish, including in tissues external to the GITs, are examined in a separate manuscript.

Overall Exposure Landscape. Below, we discuss the exposure landscape (reporting the average over time and across depths where relevant) for the highest nominal concentration (29,240 particles/L) treatment only, where we feel most confident about measured concentrations and can scale up results to the mesocosm-scale. Over the course of the experiment, 0.9% (±0.7%) of the plastic we added to the mesocosms was detected in the water samples. Thus, about 99% of the plastic was elsewhere: floating on the surface, attached to the biofilm on the walls, on the bottom, in zooplankton, in fish, or escaped via wind and waves. Scaling up the average biofilm concentrations to the area of the mesocosm walls, wall-attached biofilm accounts for 0.4% (±0.6%) of the added plastic. In the zooplankton, if we assume all taxa consume the average amount per individual measured in the five taxa, we observed 0.01% of the added plastic. We acknowledge our zooplankton data did not include all taxa, or particles <53 μm in size, so these data are conservative. In the fish, we observed 0.0001% of the added plastic. Across all matrices, we account for <1.5% of the added plastic (Figure 4). Based on our visual observations, we believe that most of the remaining microplastics were on the bottom and within the surface slick. This suggests that organisms that feed from the surface and benthos will have the greatest exposure.

Upon adding the microplastics to the mesocosms, we saw the PET sink immediately (see Supporting Information Videos). Furthermore, when we removed the mesocosms, we saw PET distributed heterogeneously on the bottom, as if they had deposited close to where we added them at the surface. This is logical based on its negative buoyancy and consistent with the very low concentrations of PET across our samples. We generally only observed PET in fish-demonstrating a need to measure benthic concentrations in the future to fully assess their exposure landscape. Similar to PET, we observed some PS sinking from the surface upon addition (see Supporting Information Videos). At the surface, we observed a much smaller PS surface slick, which appeared to be gone by 72 h. PS

https://doi.org/10.1021/acs.est.3c08990
Environ. Sci. Technol. 2024, 58, 7998−8008

is denser than water but close to neutrally buoyant. It is likely that the larger PS particles deposited rapidly, whereas the smaller particles deposited more slowly, remaining at the surface and in the water column for a longer period of time than PET. The concentrations observed in the water column confirm these particles sink (Figure S9). For PE, we observed many of the particles in a surface slick at the beginning of the experiment (see Supporting Information), which decreased in size over time. The surface slick moved around the surface of the mesocosm in accordance with the prevailing wind. The fairly consistent concentrations of microplastics in the water column over time, combined with a steady decrease in the surface slick area, suggest a steady sinking of PE particles from the surface to the biofilm on the walls and to the bottom (we predict that the vast majority likely ended up at the bottom). Some PE particles from the surface may also have been lost to wind and waves.

Although there are improvements to be made in future studies, it is unlikely that deficiencies in our sampling and laboratory methods used for the compartments sampled can account for the rest of the microplastics added to each mesocosm. Our laboratory analyses had sufficient recovery and low procedural contamination. For sampling, we feel confident in observations from our highest treatment based on the observed patterns. In the medium and low concentration treatments, we suggest future analyses would benefit from collecting greater volumes of water and larger areas of wall material. Moreover, we did not measure particles less than 53 μm. For zooplankton, previous studies indicate that the sizes of preferred food by zooplankton are typically <53 μm,[54] and thus the amounts per individual are likely an underestimate. For fish, we are not reporting amounts beyond the GITs. Future studies will benefit from quantifying all pools of microplastic in experimental mesocosms, including careful assessments of spatial and temporal heterogeneity of microplastic accumulations in surface and benthic compartments.

In future years, informed by this experiment, we will improve our sampling design to increase our understanding of the microplastic exposure landscape within our pELAstic project. This will include more representative sampling methods and further coverage of the missing compartments. Other laboratory and field experiments would benefit from the same, as microplastics do not behave like other substances that mix uniformly into the water column.[55] Instead, they behave like particles (with a very diverse suite of shapes, sizes, and densities)—and future studies should design their experiments and sampling campaigns with this in mind. Further work is needed to better measure and understand the exposure landscape to fully express the dose and bioavailability to organisms. This is especially important for ecotoxicity experiments aiming to study ecologically relevant effects. The complex fate of microplastics and how it varies based on particle characteristics (e.g., morphology, polymer, size) must be considered. Considering the exposure landscape is likely to affect the experimental design and sampling efforts of microplastics reseearch moving forward.

■ ASSOCIATED CONTENT

Supporting Information

The Supporting Information is available free of charge at https://pubs.acs.org/doi/10.1021/acs.est.3c08990. The raw Supplementary Data can be obtained via this link: https://doi.org/10.5683/SP3/WNVCCC.

Additional experimental details, materials, and methods, and data, including photographs (PDF)

Video of experimental setup (ZIP)

■ AUTHOR INFORMATION

Corresponding Author

Chelsea M. Rochman − *Department of Ecology and Evolutionary Biology, University of Toronto, Toronto, Ontario M5S 3B2, Canada;* orcid.org/0000-0002-7624-711X; Email: chelsea.rochman@utoronto.ca

Authors

Kennedy Bucci − *Department of Ecology and Evolutionary Biology, University of Toronto, Toronto, Ontario M5S 3B2, Canada;* orcid.org/0000-0003-0560-0059

Desiree Langenfeld − *International Institute for Sustainable Development Experimental Lakes Area, Winnipeg, Manitoba R3B 0T4, Canada; Department of Entomology, University of Manitoba, Winnipeg, Manitoba MB R3T 2N2, Canada*

Rachel McNamee − *Biology Department, University of Waterloo, Waterloo, Ontario ON N2L 3G1, Canada*

Cody Veneruzzo − *Department of Biology, Lakehead University, Thunder Bay, Ontario ON P7B 5E1, Canada*

Garth A. Covernton − *Department of Ecology and Evolutionary Biology, University of Toronto, Toronto, Ontario M5S 3B2, Canada*

Gloria H. Y. Gao − *Department of Ecology and Evolutionary Biology, University of Toronto, Toronto, Ontario M5S 3B2, Canada*

Mira Ghosh − *Department of Ecology and Evolutionary Biology, University of Toronto, Toronto, Ontario M5S 3B2, Canada*

Rachel N. Cable − *Department of Ecology and Evolutionary Biology, University of Michigan, Ann Arbor, Michigan 48109, United States;* orcid.org/0000-0002-5859-5612

Ludovic Hermabessiere − *Department of Ecology and Evolutionary Biology, University of Toronto, Toronto, Ontario M5S 3B2, Canada*

Raul Lazcano − *Department of Biology, Loyola University Chicago, Chicago, Illinois 60611, United States*

Michael J. Paterson − *International Institute for Sustainable Development Experimental Lakes Area, Winnipeg, Manitoba R3B 0T4, Canada; Department of Entomology, University of Manitoba, Winnipeg, Manitoba MB R3T 2N2, Canada*

Michael D. Rennie − *International Institute for Sustainable Development Experimental Lakes Area, Winnipeg, Manitoba R3B 0T4, Canada; Department of Biology, Lakehead University, Thunder Bay, Ontario ON P7B 5E1, Canada;* orcid.org/0000-0001-7533-4759

Rebecca C. Rooney − *Biology Department, University of Waterloo, Waterloo, Ontario ON N2L 3G1, Canada*

Paul Helm − *Environmental Monitoring and Reporting Branch, Ontario Ministry of the Environment, Conservation and Parks, Toronto, Ontario M9P 3 V6, Canada;* orcid.org/0000-0002-7462-4217

Melissa B. Duhaime − *Department of Ecology and Evolutionary Biology, University of Michigan, Ann Arbor, Michigan 48109, United States*

Timothy Hoellein − *Department of Biology, Loyola University Chicago, Chicago, Illinois 60611, United States*

Kenneth M. Jeffries − *Department of Biological Sciences, University of Manitoba, Winnipeg, Manitoba MB R3T 2N2, Canada*

https://doi.org/10.1021/acs.est.3c08990
Environ. Sci. Technol. 2024, 58, 7998−8008

Matthew J. Hoffman − *School of Mathematics and Statistics, Rochester Institute of Technology, Rochester, New York 14623, United States*

Diane M. Orihel − *Department of Biology and School of Environmental Studies, Queen's University, Kingston, Ontario K7L 3N6, Canada;* orcid.org/0000-0002-6933-3650

Jennifer F. Provencher − *Environment and Climate Change Canada, National Wildlife Research Centre, Ottawa K1A 0H3, Canada;* orcid.org/0000-0002-4972-2034

Complete contact information is available at: https://pubs.acs.org/10.1021/acs.est.3c08990

Notes

The authors declare no competing financial interest.

■ ACKNOWLEDGMENTS

This is Contribution #2 of the pELAstic project. Thanks to many who helped in the field (T. Rodriguez, C. Currie, H. Jovanovic, A. Ross, W. Dombroskie) and staff at IISD-ELA, including the fish crew (especially L. Hayhurst and L. Hrenchuk) and the chemistry laboratory (especially S. Havens). This project was supported by a DFO NCAG grant and funding from Loblaws, an NSERC Discovery and Ontario Early Researcher Award to C.M.R., a CRC and NSERC Discovery to M.D.R., an ECCC IKPP awarded to L.H., K.M.J., and C.M.R., a University of Toronto Faculty of Arts and Science Fellowship to G.A.C., and the IISD-ELA Graduate Student Fund and Jim and Leney Richardson Student Grants. Thanks to the three reviewers who offered thoughtful comments to improve our manuscript.

■ REFERENCES

(1) Brahney, J.; Mahowald, N.; Prank, M.; Cornwell, G.; Klimont, Z.; Matsui, H.; Prather, K. A. Constraining the atmospheric limb of the plastic cycle. *Proc. Natl. Acad. Sci. U.S.A.* **2021**, *118* (16), No. e2020719118.

(2) Bergmann, M.; Mützel, S.; Primpke, S.; Tekman, M. B.; Trachsel, J.; Gerdts, G. White and wonderful? Microplastics prevail in snow from the Alps to the Arctic. *Sci. Adv.* **2019**, *5* (8), No. eaax1157.

(3) Dees, J. P.; Ateia, M.; Sanchez, D. L. Microplastics and their degradation products in surface waters: A missing piece of the global carbon cycle puzzle. *ACS ES&T Water* **2021**, *1* (2), 214−216.

(4) Zhu, X. The plastic cycle−an unknown branch of the carbon cycle. *Front. Mar. Sci.* **2021**, *7*, 1227.

(5) Worm, B.; Lotze, H. K.; Jubinville, I.; Wilcox, C.; Jambeck, J. Plastic as a persistent marine pollutant. *Annu. Rev. Environ. Resour.* **2017**, *42* (1), 1−26.

(6) Rochman, C. M.; Hoellein, T. The global odyssey of plastic pollution. *Science* **2020**, *368* (6496), 1184−1185.

(7) Lohmann, R.; Corrigan, B. P.; Howsam, M.; Jones, K. C.; Ockenden, W. A. Further developments in the use of semipermeable membrane devices (SPMDs) as passive air samplers for persistent organic pollutants: field application in a spatial survey of PCDD/Fs and PAHs. *Environ. Sci. Technol.* **2001**, *35* (12), 2576−2582.

(8) Chen, J.; Harner, T.; Ding, G.; Quan, X.; Schramm, K. W.; Kettrup, A. Universal predictive models on octanol-air partition coefficients at different temperatures for persistent organic pollutants. *Environ. Toxicol. Chem.* **2004**, *23* (10), 2309−2317.

(9) Daily, J.; Hoffman, M. J. Modeling the three-dimensional transport and distribution of multiple microplastic polymer types in Lake Erie. *Mar. Pollut. Bull.* **2020**, *154*, 111024.

(10) Daily, J.; Tyler, A. C.; Hoffman, M. J. Modeling three-dimensional transport of microplastics and impacts of biofouling in Lake Erie and Lake Ontario. *J. Great Lake. Res.* **2022**, *48* (5), 1180−1190.

(11) Khatmullina, L.; Chubarenko, I. Transport of marine microplastic particles: why is it so difficult to predict? *Anthropocene Coast* **2019**, *2* (1), 293−305.

(12) Cable, R. N.; Beletsky, D.; Beletsky, R.; Wigginton, K.; Locke, B. W.; Duhaime, M. B. Distribution and modeled transport of plastic pollution in the Great Lakes, the world's largest freshwater resource. *Front. Environ. Sci.* **2017**, *5*, 45.

(13) Choy, C. A.; Robison, B. H.; Gagne, T. O.; Erwin, B.; Firl, E.; Halden, R. U.; Hamilton, J. A.; Katija, K.; Lisin, S. E.; Rolsky, C.; S Van Houtan, K. The vertical distribution and biological transport of marine microplastics across the epipelagic and mesopelagic water column. *Sci. Rep.* **2019**, *9* (1), 7843−7849.

(14) Turner, S.; Horton, A. A.; Rose, N. L.; Hall, C. A temporal sediment record of microplastics in an urban lake, London, UK. *J. Paleolimnol.* **2019**, *61* (4), 449−462.

(15) Xu, N.; Zhu, Z.; Gao, W.; Shao, D.; Li, S.; Zhu, Q.; Fan, Z.; Cai, Y.; Yang, Z. Effects of waves, burial depth and material density on microplastic retention in coastal sediments. *Sci. Total Environ.* **2023**, *864*, 161093.

(16) McIlwraith, H. K.; Kim, J.; Helm, P.; Bhavsar, S. P.; Metzger, J. S.; Rochman, C. M. Evidence of microplastic translocation in wild-caught fish and implications for microplastic accumulation dynamics in food webs. *Environ. Sci. Technol.* **2021**, *55* (18), 12372−12382.

(17) Covernton, G. A.; Cox, K. D.; Fleming, W. L.; Buirs, B. M.; Davies, H. L.; Juanes, F.; Dudas, S. E.; Dower, J. F. Large size (> 100-μm) microplastics are not biomagnifying in coastal marine food webs of British Columbia, Canada. *Ecol. Appl.* **2022**, *32*, No. e2654.

(18) Waldschläger, K.; Schüttrumpf, H. Effects of particle properties on the settling and rise velocities of microplastics in freshwater under laboratory conditions. *Environ. Sci. Technol.* **2019**, *53* (4), 1958−1966.

(19) Bulleri, F.; Ravaglioli, C.; Anselmi, S.; Renzi, M. The sea cucumber Holothuria tubulosa does not reduce the size of microplastics but enhances their resuspension in the water column. *Sci. Total Environ.* **2021**, *781*, 146650.

(20) Efimova, I.; Bagaeva, M.; Bagaev, A.; Kileso, A.; Chubarenko, I. P. Secondary microplastics generation in the sea swash zone with coarse bottom sediments: laboratory experiments. *Front. Mar. Sci.* **2018**, *5*, 313.

(21) Lobelle, D.; Kooi, M.; Koelmans, A. A.; Laufkötter, C.; Jongedijk, C. E.; Kehl, C.; van Sebille, E. Global modeled sinking characteristics of biofouled microplastic. *J. Geophys. Res.: Oceans* **2021**, *126* (4), No. e2020JC017098.

(22) Van Sebille, E.; Wilcox, C.; Lebreton, L.; Maximenko, N.; Hardesty, B. D.; Van Franeker, J. A.; Eriksen, M.; Siegel, D.; Galgani, F.; Law, K. L. A global inventory of small floating plastic debris. *Environ. Res. Lett.* **2015**, *10* (12), 124006.

(23) Koelmans, A. A.; Kooi, M.; Law, K. L.; Van Sebille, E. All is not lost: deriving a top-down mass budget of plastic at sea. *Environ. Res. Lett.* **2017**, *12* (11), 114028.

(24) Wang, L.; Li, P.; Zhang, Q.; Wu, W. M.; Luo, J.; Hou, D. Modeling the conditional fragmentation-induced microplastic distribution. *Environ. Sci. Technol.* **2021**, *55* (9), 6012−6021.

(25) Kidd, K. A.; Blanchfield, P. J.; Mills, K. H.; Palace, V. P.; Evans, R. E.; Lazorchak, J. M.; Flick, R. W. Collapse of a fish population after exposure to a synthetic estrogen. *Proc. Natl. Acad. Sci. U.S.A.* **2007**, *104* (21), 8897−8901.

(26) Oswald, C. J.; Heyes, A.; Branfireun, B. A. Fate and transport of ambient mercury and applied mercury isotope in terrestrial upland soils: insights from the METAALICUS watershed. *Environ. Sci. Technol.* **2014**, *48* (2), 1023−1031.

(27) Orihel, D. M.; Bisbicos, T.; Darling, C. T.; Dupuis, A. P.; Williamson, M.; Muir, D. C. Probing the debromination of the flame retardant decabromodiphenyl ether in sediments of a boreal lake. *Environ. Toxicol. Chem.* **2016**, *35* (3), 573−583.

(28) Hoellein, T. J.; Shogren, A. J.; Tank, J. L.; Risteca, P.; Kelly, J. J. Microplastic deposition velocity in streams follows patterns for naturally occurring allochthonous particles. *Sci. Rep.* **2019**, *9*, 3740.

(29) Schindler, D. W. A personal history of the Experimental Lakes ProjectThis paper is part of the series "Forty Years of Aquatic

Research at the Experimental Lakes Area". *Can. J. Fish. Aquat. Sci.* **2009**, *66* (11), 1837−1847.
(30) Schindler, D. W.; Armstrong, F. A. J.; Holmgren, S. K.; Brunskill, G. J. Eutrophication of Lake 227, Experimental Lakes Area, northwestern Ontario, by addition of phosphate and nitrate. *J. Fish. Res. Board Can.* **1971**, *28* (11), 1763−1782.
(31) Schindler, D. W.; Bayley, S. E.; Parker, B. R.; Beaty, K. G.; Cruikshank, D. R.; Fee, E. J.; Schindler, E. U.; Stainton, M. P. The effects of climatic warming on the properties of boreal lakes and streams at the Experimental Lakes Area, northwestern Ontario. *Limnol. Oceanogr.* **1996**, *41* (5), 1004−1017.
(32) Schindler, D. W.; Wagemann, R.; Cook, R. B.; Ruszczynski, T.; Prokopowich, J. Experimental acidification of Lake 223, Experimental Lakes Area: Background data and the first three years of acidification. *Can. J. Fish. Aquat. Sci.* **1980**, *37* (3), 342−354.
(33) Blanchfield, P. J.; Rudd, J. W.; Hrenchuk, L. E.; Amyot, M.; Babiarz, C. L.; Beaty, K. G.; Bodaly, R. A. D.; Branfireun, B. A.; Gilmour, C. C.; Graydon, J. A.; Hall, B. D.; et al. Experimental evidence for recovery of mercury-contaminated fish populations. *Nature* **2022**, *601* (7891), 74−78.
(34) Rodriguez-Gil, J. L.; Stoyanovich, S.; Hanson, M. L.; Hollebone, B.; Orihel, D. M.; Palace, V.; Faragher, R.; Mirnaghi, F. S.; Shah, K.; Yang, Z.; Black, T. A.; et al. Simulating diluted bitumen spills in boreal lake limnocorrals-Part 1: Experimental design and responses of hydrocarbons, metals, and water quality parameters. *Sci. Total Environ.* **2021**, *790*, 148537.
(35) Hayhurst, L. D.; Martin, J. D.; Wallace, S. J.; Langlois, V. S.; Xenopoulos, M. A.; Metcalfe, C. D.; Rennie, M. D. Multi-level responses of yellow perch (Perca flavescens) to a whole-lake nanosilver addition study. *Arch. Environ. Contam. Toxicol.* **2020**, *79*, 283−297.
(36) Boisclair, D.; Leggett, W. C. Among-population variability of fish growth: I. Influence of the quantity of food consumed. *Can. J. Fish. Aquat. Sci.* **1989**, *46* (3), 457−467.
(37) Hataley, E. K.; McIlwraith, H. K.; Roy, D.; Rochman, C. M. Towards a management strategy for microplastic pollution in the Laurentian Great Lakes—ecological risk assessment and management (part 2). *Can. J. Fish. Aquat. Sci.* **2023**, *80*, 1669−1678.
(38) Koelmans, A. A.; Redondo-Hasselerharm, P. E.; Mohamed Nor, N. H.; Kooi, M. Solving the nonalignment of methods and approaches used in microplastic research to consistently characterize risk. *Environ. Sci. Technol.* **2020**, *54* (19), 12307−12315.
(39) Kooi, M.; Primpke, S.; Mintenig, S. M.; Lorenz, C.; Gerdts, G.; Koelmans, A. A. Characterizing the multidimensionality of microplastics across environmental compartments. *Water Res.* **2021**, *202*, 117429.
(40) Prepas, E. Sugar-frosted Daphnia: an improved fixation technique for Cladocera. *Limnol. Oceanogr.* **1978**, *23*, 557−559.
(41) Gannon, J. E.; Gannon, S. A. Observations On the Narcotization of Crustacean Zooplankton 1). *Crustaceana* **1975**, *28*, 220−224.
(42) Munno, K.; De Frond, H.; O'Donnell, B.; Rochman, C. M. Increasing the accessibility for characterizing microplastics: introducing new application-based and spectral libraries of plastic particles (SLoPP and SLoPP-E). *Anal. Chem.* **2020**, *92* (3), 2443−2451.
(43) De Frond, H.; Rubinovitz, R.; Rochman, C. M. μATR-FTIR Spectral Libraries of Plastic Particles (FLOPP and FLOPP-e) for the Analysis of Microplastics. *Anal. Chem.* **2021**, *93* (48), 15878−15885.
(44) R Core Team. *R: A Language and Environment for Statistical Computing*; R Foundation for Statistical Computing. 2022, https://www.R-project.org/.
(45) Brooks, M. E.; Kristensen, K.; BenthemMagnusson, K. A.; Berg, C.; Nielsen, A.; Skaug, H.; Mächler, M.; Bolker, B.; Bolker, B. M. glmmTMB Balances Speed and Flexibility Among Packages for Zero-inflated Generalized Linear Mixed Modeling. *R J.* **2017**, *9* (2), 378−400.
(46) Hartig, F. DHARMa: Residual Diagnostics for Hierarchical (Multi-Level/Mixed) Regression Models. 2022, https://CRAN.R-project.org/package=DHARMa accessed Feb 15, 2024.
(47) Lenth, R. V. Emmeans: Estimated Marginal Means, Aka Least-Squares Means. 2022, https://CRAN.R-project.org/package=emmeans accessed Feb 15, 2024.
(48) Lüdecke, D. ggeffects: Tidy Data Frames of Marginal Effects from Regression Models. *J. Open Source Softw.* **2018**, *3* (26), 772.
(49) Hung, C.; Klasios, N.; Zhu, X.; Sedlak, M.; Sutton, R.; Rochman, C. M. Methods matter: methods for sampling microplastic and other anthropogenic particles and their implications for monitoring and ecological risk assessment. *Integrated Environ. Assess. Manag.* **2021**, *17* (1), 282−291.
(50) Kooi, M.; Koelmans, A. A. Simplifying microplastic via continuous probability distributions for size, shape, and density. *Environ. Sci. Technol. Lett.* **2019**, *6* (9), 551−557.
(51) Semcesen, P. O.; Wells, M. G. Biofilm growth on buoyant microplastics leads to changes in settling rates: implications for microplastic retention in the Great Lakes. *Mar. Pollut. Bull.* **2021**, *170*, 112573.
(52) Elagami, H.; Frei, S.; Boos, J. P.; Trommer, G.; Gilfedder, B. S. Quantifying microplastic residence times in lakes using mesocosm experiments and transport modelling. *Water Res.* **2023**, *229*, 119463.
(53) Steer, M.; Cole, M.; Thompson, R. C.; Lindeque, P. K. Microplastic ingestion in fish larvae in the western English Channel. *Environ. Pollut.* **2017**, *226*, 250−259.
(54) Sterner, R. W. The role of grazers in phytoplankton succession. *Plankton Ecology: Succession in Plankton Communities*; Sommer, U., ed.; Springer-Verlag: Berlin, 1989; pp 107−170.
(55) Paul-Pont, I.; Tallec, K.; Gonzalez-Fernandez, C.; Lambert, C.; Vincent, D.; Mazurais, D.; Zambonino-Infante, J. L.; Brotons, G.; Lagarde, F.; Fabioux, C.; Soudant, P.; et al. Constraints and priorities for conducting experimental exposures of marine organisms to microplastics. *Front. Mar. Sci.* **2018**, *5*, 252.

https://doi.org/10.1021/acs.est.3c08990
Environ. Sci. Technol. 2024, 58, 7998−8008